

# Dual-Band Handset Antenna Based on Multi-Branch Monopole for LTE/WWAN Applications

<sup>1</sup>Tzu-Heng Cheng, <sup>1</sup>Jen-Kuei Tsai, <sup>1</sup>Wan-Ting Hung, and <sup>2</sup>Shih-Yuan Chen

<sup>1</sup>Graduate Institute of Communication Engineering and <sup>2</sup>Department of Electrical Engineering,  
National Taiwan University, Taipei 10617, Taiwan

**Abstract** - A single-feed compact dual-band antenna based on multi-branch monopole structure is proposed for LTE/WWAN handset applications. Its operational principles are illustrated via a series of parametric analyses, showing the origin and characteristic of each of the resonant modes. For verification, a prototype antenna was built, and the measured performance agrees well with those simulated.

**Index Terms** — Dual-band antennas, handset antennas.

## 1. Introduction

Several compact dual-band designs have been proposed for handset applications [1]-[4]. To achieve the dual-band operation, hybrid antenna structures have been commonly used. However, because of the limited available area of the antenna, strong coupling between constituent radiators exists in such designs such that the synthesis of the two operating bands has never been an easy task. Moreover, lumped reactive elements have also been exploited in some designs to improve the impedance matching [3]. In this paper, a very simple dual-band handset antenna that requires no lumped elements is proposed. Our proposed antenna is formed by three short strips and a longer folded thin strip. The three short strips respectively generate the three anti-resonances at the upper band, and the longer folded thin strip produces the anti-resonance at the lower band. All the four resonant frequencies can be almost independently controlled by tuning the corresponding strip lengths, which largely facilitates the dual-band matching of our proposed antenna.

## 2. Antenna Structure and Design

The configuration of the proposed antenna with a total size of  $55 \times 10 \times 5 \text{ mm}^3$  is depicted in Fig. 1. The antenna is integrated with and placed near the upper edge of a  $70 \times 120 \text{ mm}^2$  rectangular conducting ground plane and a 0.6-mm-thick supporting substrate FR4 ( $\epsilon_r = 4.4$ ). As shown in Fig. 1(b), the parameters,  $L_1$ ,  $L_2$ , and  $L_3$ , represent the lengths of Strips 1, 2, and 3, respectively. These metallic strips generate three independent resonant modes within the upper desired band (1710-2170 MHz) and together form a wide impedance bandwidth. To maintain the wide bandwidth and radiation efficiency within the upper band, Strips 1-3 are made straight without meandering or folding. Meanwhile, as shown in Fig. 1(b), an extra folded thin strip extends from Strip 2, resulting in a total length of about  $(L_2 + 73)$  mm, and they together produce an additional resonant mode at the lower band (700-800 MHz). Besides, the usage of the folded thin strip also improves the impedance matching at the upper band. Note

that this thin strip should be properly folded to avoid strong electric coupling with strip 1 near its open end while keeping a compact size. The narrow (0.3 mm) gap between the end of the folded thin strip and ground plane acts as a capacitor loaded at the end of an open-circuited strip. Besides, as shown in Fig. 1(b), a  $55 \times 5 \text{ mm}^2$  vertical copper wall that is rendered parallel to the x-y plane is added to the uppermost arm of the folded thin strip to further enlarge the bandwidth of the lower band. To facilitate antenna testing and enhance the robustness of measurement setup, a  $50\Omega$  microstrip line that can be printed on the same FR4 slab as the antenna was adopted as feedline in both the simulation model and fabricated prototype as shown in Fig. 1(a).

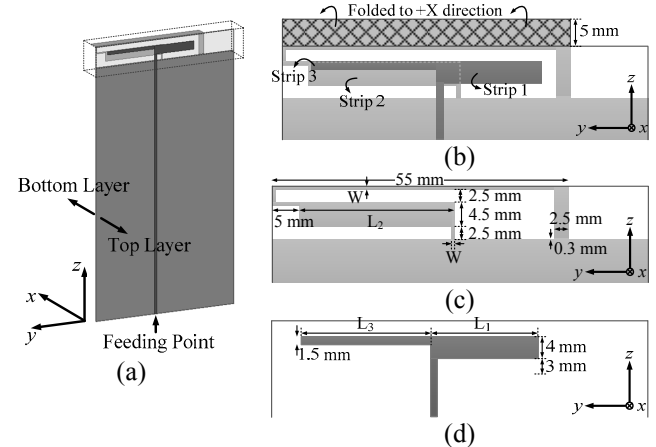


Fig. 1. (a) Perspective view of the proposed antenna and ground plane. (b) Enlarged view of the antenna part and the layouts of the (c) bottom and (d) top metallic layer. (Widths of all thin strips in (c) are  $W = 0.5 \text{ mm}$ .)

To investigate the effects of Strips 1-3 and the folded thin strip on the resonant modes, a series of parametric analyses were performed, and the results are shown in Fig. 2. First, consider a simplified structure without Strip 3 and the folded thin strip and with  $L_1 < L_2$ . Two anti-resonances associated respectively with the fundamental monopole modes of Strips 1 and 2 can be observed in Fig. 2(a) and (b). The anti-resonance around 1700 MHz is caused by Strip 2, while that above 2500 MHz is due to Strip 1. Clearly, by increasing  $L_1$ , the frequency of the higher resonant mode can be lowered without shifting the lower one. Similarly, by increasing  $L_2$ , the frequency of the lower resonance can be lowered without shifting the higher one. In short, these two resonances can be adjusted easily and independently by tuning  $L_1$  and  $L_2$ . Next, as shown in Fig. 2(c), Strip 3 is now added for it can enhance

the impedance matching and widen the bandwidth. It produces an additional resonance (around 2000 MHz) between the two resonances caused by Strips 1 and 2. Its resonant frequency can also be independently controlled by tuning  $L_3$ . Note that, in the above two simplified designs, no resonance occurs within the lower desired band. So, lastly, the folded thin strip was added to the open end of Strip 2, the longest among Strips 1-3, to produce a resonance inside the lower band without affecting the three resonances in the upper band as shown in Fig. 2(d).

### 3. Simulated and Measured Results

A prototype antenna with  $L_1 = 20.0$  mm,  $L_2 = 28.9$  mm, and  $L_3 = 24.0$  mm was fabricated and tested. A photograph of the fabricated prototype is shown in Fig. 3. The simulated and measured  $|S_{11}|$  responses are plotted in Fig. 4(a), and they are in good agreement. The simulated and measured 6-dB return loss bandwidths are respectively 703-812 MHz and 726-821 MHz at the lower band and 1673-2436 MHz and 1709-2455 MHz at the upper band. Clearly, typical LTE/WWAN bands are covered. Fig. 4(b) shows the antenna efficiencies of the prototype. The measured peak antenna efficiencies are higher than 50% and 65% at the lower and upper bands, respectively. Moreover, the simulated and measured radiation patterns at three sample frequencies are plotted in Fig. 5. Again, they all agree well with each other. The measured peak gains are  $-0.93$  dBi at 750 MHz,  $2.64$  dBi at 1700 MHz, and  $0.31$  dBi at 2000 MHz.

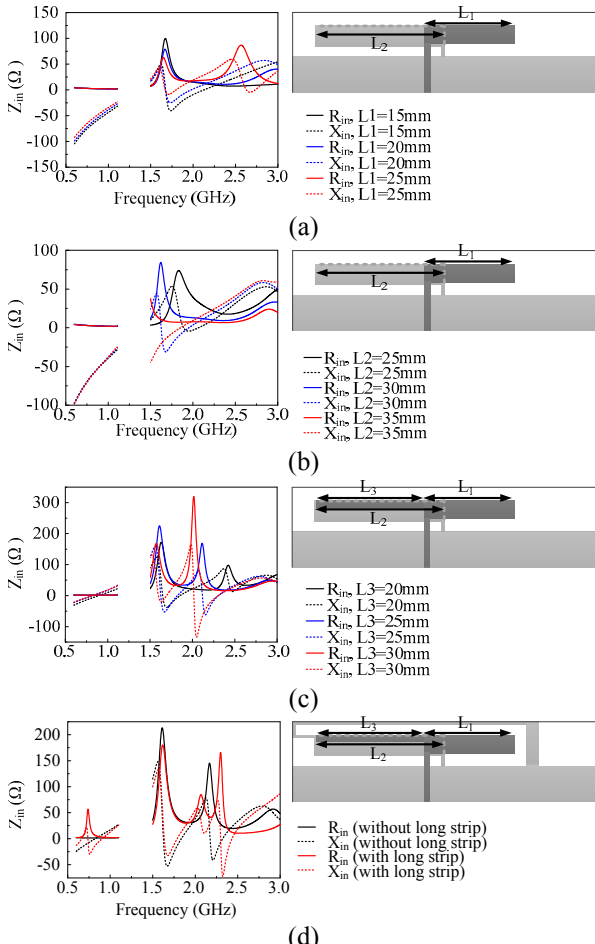


Fig. 2. Impedance responses of the simplified designs for various (a)  $L_1$ , (b)  $L_2$ , and (c)  $L_3$  and (d) the proposed design

with and without the folded thin strip.



Fig. 3. Photograph of the prototype antenna.

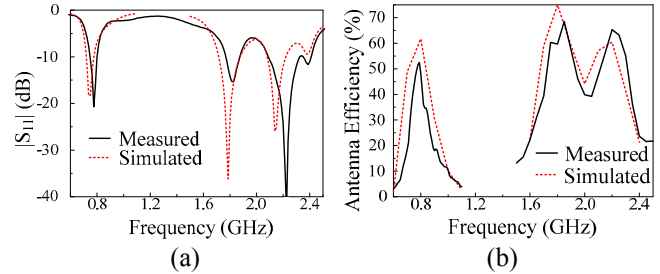


Fig. 4. Simulated and measured (a)  $|S_{11}|$  and (b) antenna efficiencies of the prototype antenna.

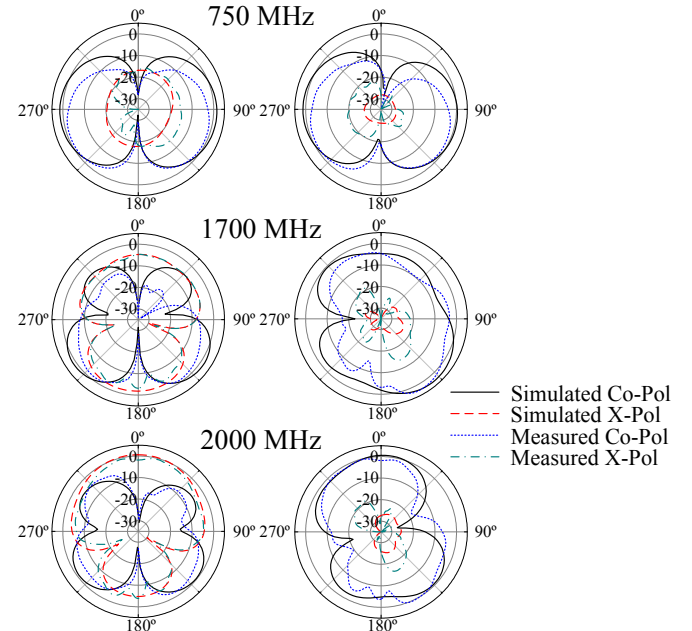


Fig. 5. Simulated and measured radiation patterns at three sample frequencies. (Left: x-z plane; right: y-z plane).

### Acknowledgment

This work was supported by the Ministry of Science and Technology, Taiwan, under Contract: MOST 104-2628-E-002-006-MY2.

### References

- [1] P.-W. Lin and K.-L. Wong, "Internal WWAN handset antenna formed by a monopole strip radiator and a clearance region thereof as monopole slot radiator," *Proc. Int. Symp. Antennas and Propagat.*, pp. 1361-1364, Oct. 2012.
- [2] F.-H. Chu and K.-L. Wong, "Simple folded monopole slot antenna for penta-band clamshell mobile phone application," *IEEE Trans. Antennas Propag.*, vol. 57, pp. 3680-3684, Nov. 2009.
- [3] K.-L. Wong and Y.-C. Chen, "Small-Size Hybrid Loop/Open-Slot Antenna for the LTE Smartphone," *IEEE Trans. Antennas Propag.*, vol. 63, pp. 5837-5841, Dec. 2015.
- [4] Y.-L. Shih, B.-H. Wang, Y.-J. Lu, J.-C. Cheng, S.-Y. Chen, and P. Hsu, "Capacitively-loaded loop antenna for multi-band mobile handsets," *Proc. Int. Workshop Antenna Technol.*, pp. 239-242, 2008.